IEEE Access
Multidisciplinary | Rapid Review | Open Access Journal

Received January 14, 2020, accepted January 24, 2020, date of publication February 10, 2020, date of current version February 17, 2020.

Digital Object Identifier 10.1109/ACCESS.2020.2972739

Filtering Power Amplifier With Up to 4th Harmonic Suppression

XIAOBO QI AND FEI XIAO, (Member, IEEE)
School of Electronic Science and Engineering, University of Electronic Science and Technology of China, Chengdu 611731, China
Corresponding author: Fei Xiao (fxiao@uestc.edu.cn)

This work was supported by the National Natural Science Foundation of China under Project 61671111.

ABSTRACT Unlike conventional conception that power amplifier and filter are regarded as two separate components and designed separately, this paper presents a high efficiency power amplifier with filtering capability, which is called filtering power amplifier. The proposed power amplifier integrates a bandpass filter as output matching network so that entire size is reduced to some extent. The filter will play the role of filtering and impedance matching simultaneously, and thus high-order harmonics are suppressed for output of the filtering power amplifier. For demonstration, an example of filtering power amplifier was designed, fabricated and measured. The measurement shows that it is featured by highly-selective bandpass response and good out-of-band performance. As high as 46.2 dB suppression can be achieved and extended over the forth-order harmonic. The example also retains the advantages of high efficiency and output power. The maximum output power can reach 40.5 dBm, and the maximum power-added efficiency is as high as 62%.

INDEX TERMS Bandpass filter, efficiency, filtering power amplifier, harmonic suppression.

I. INTRODUCTION

Power amplifiers (PA) is the key components in wireless communication systems, and its performance is decisive for system quality and energy consumption [1]. At present, how to further improve their efficiency and bandwidth is still concerned by researchers. For example, Class-F PAs are designed by using harmonic control methods to achieve higher efficiency in [2]–[5]. Reference [6] designs a high efficiency class-E PA by analyzing the DC I-V curve of the actual device. Reference [7] presents a high efficiency PA using real-frequency matching technology. A design approach based on optimized impedance solution continuum for broadband PA is proposed in [8]. In [9], a design method for dual-frequency Doherty power amplifier (DPA) using dual-frequency phase shift lines to improve performance is proposed. Reference [10] discusses a high-efficiency asymmetric class-F/F^{-1} DPA, which consists of a class-F^{-1} carrier amplifier and a class-F peak amplifier. In [11], a wideband PA is designed, whose output matching network is composed of 16 identical branch structures loaded on the ring resonator.

In practical application, clean spectrum output from PA is required. Conventionally, a separate filter is cascaded after PA for purifying output spectrum [12]–[15]. So, conventional filter and PA are regarded as two separate components and designed separately. However, such treatment will unfortunately lead to some problems such as large size and mismatching. Recently, [16] explores the combination of both for seize reduction. Reference [17] proposes a schematic in which a dielectric resonator and a PA are integrated. Reference [18] proposes a high-power PA matched by bandpass filter for long term evolution applications. Reference [19] proposes a high efficiency PA with good bandpass response.

For purpose of whole performance optimization and miniaturization, this paper proposes a PA incorporating a bandpass filter as output matching network. The filter plays the role of filtering and impedance matching simultaneously. Such is called filtering power amplifier (FPA) for simplicity. The measurement demonstrates that the proposed FPA is featured by sharp selectivity and high harmonic suppression. At the same time, it still retains the advantages of high power-added efficiency and wide bandwidth.

II. ANALYSIS AND DESIGN OF FILTERING POWER AMPLIFIER

Apart from bandwidth and efficiency, out-of-band performance of PA is also important. Any unwanted noises or interferences coming either from outside or inside PA will unfortunately deteriorate whole performance. Therefore, it is necessary to suppress those and not let them enter

The associate editor coordinating the review of this manuscript and approving it for publication was Jing Xia.

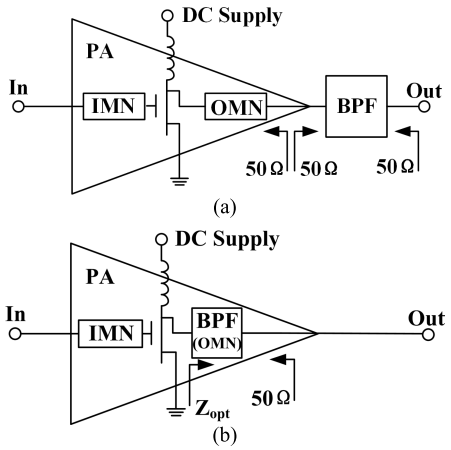

FIGURE 1. Schematic diagram. (a) Conventional separate PA and Filter. (b) FPA.

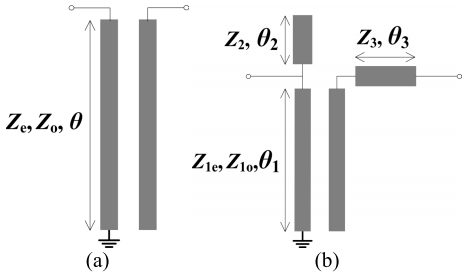

FIGURE 2. Parallel-coupled two-line section and its variation form. (a) Configuration of parallel-coupled two-line section and (b) Its variation form.

next component. Conventionally, a filter is cascaded after PA for such purpose, as shown in Fig. 1(a). In Fig. 1(a), IMN denotes input matching network and OMN denotes output matching network, which belong to PA. BPF denotes bandpass filter. Conventionally, PA and bandpass filter are regarded as two separate components, and then designed separately.

In order to reduce size and achieve performance optimization, this paper focuses on the integration design of PA and filter, i.e., FPA, as shown in Fig. 1(b). Instead of regarding filter as a separate component, we incorporate it into PA. Apart from its frequency selection, the filter will also act as OMN for PA. Accordingly, such scheme is advantageous to size reduction and whole performance optimization. In the following, the design detail of FPA will be discussed.

A. NOVEL BANDPASS FILTER

Firstly, the parallel-coupled two-line section is considered, as shown in Fig. 2(a). According to transmission-line theory, it is described by the following ABCD matrix.

$$\begin{bmatrix} A & B \\ C & D \end{bmatrix} = \begin{bmatrix} \dfrac{Z_{0e}+Z_{0o}}{Z_{0e}-Z_{0o}} & -j\dfrac{2Z_{0e}Z_{0o}}{Z_{0e}-Z_{0o}}\cot\theta \\ -j\dfrac{2}{Z_{0e}-Z_{0o}}\cot\theta & -\dfrac{Z_{0e}+Z_{0o}}{Z_{0e}-Z_{0o}}\cot^2\theta+\dfrac{Z_{0e}-Z_{0o}}{Z_{0e}+Z_{0o}}\csc^2\theta \end{bmatrix} \quad (1)$$

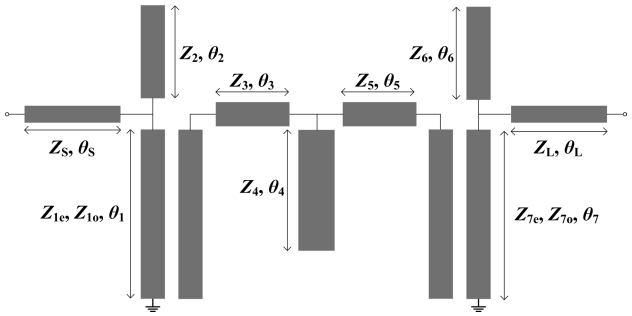

FIGURE 3. Prototype of the proposed filter.

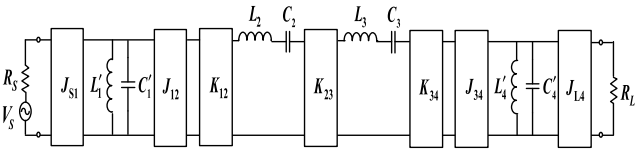

FIGURE 4. Equivalent circuit of the proposed bandpass filter.

It can be decomposed as

$$\begin{bmatrix} A & B \\ C & D \end{bmatrix} = \begin{bmatrix} 1 & 0 \\ -j\dfrac{2}{Z_{0e}+Z_{0o}}\cot\theta & 1 \end{bmatrix} \times \begin{bmatrix} \dfrac{Z_{0e}+Z_{0o}}{Z_{0e}-Z_{0o}} & 0 \\ 0 & \dfrac{Z_{0e}-Z_{0o}}{Z_{0e}+Z_{0o}} \end{bmatrix} \begin{bmatrix} 1 & -j\dfrac{2Z_{0e}Z_{0o}}{Z_{0e}+Z_{0o}}\cot\theta \\ 0 & 1 \end{bmatrix} \quad (2)$$

Obviously, it can be considered as two coupled resonators. In order to make it flexible for practical operation, its variation form in Fig. 2(b) is utilized instead. If such two structures are cascaded, a filter is formed, as shown in Fig. 3.

For the filter prototype in Fig. 3, the line section with the electric length $(\theta_1 + \theta_2)$ acts as Resonator $R1$, the one with $(\theta_1 + \theta_3)$ acts as Resonator $R2$, the one with $(\theta_5 + \theta_7)$ acts as Resonator $R3$, and the one with $(\theta_6+\theta_7)$ acts as Resonator $R4$. These electric lengths are approximately equal to $\pi/2$ at the center frequency. Thus, this filter owns four main resonances for operation. In addition, the stub with the impedance Z_4 and the electric length θ_4 acts as an impedance inverter between Resonator $R2$ and $R3$.

It is not easy to directly analyze the whole microstrip structure in Fig. 3 because mathematical expression derived by applying transmission-line theory is very complex. Instead, it is effective approach to use lumped-element equivalent circuit to represent microstrip structure. The equivalent circuit of the filter prototype is shown in Fig. 4. Resonator $R1$ is represented by the shunt $L_1'C_1'$, Resonator $R2$ by the series L_2C_2, Resonator $R3$ by the series L_3C_3, and Resonator $R4$ by the shunt $L_4'C_4'$, respectively. The line section with Z_S and θ_S acts as the source admittance inverter J_{S1}, and the one with Z_L and θ_L acts as the load admittance inverter J_{S4},

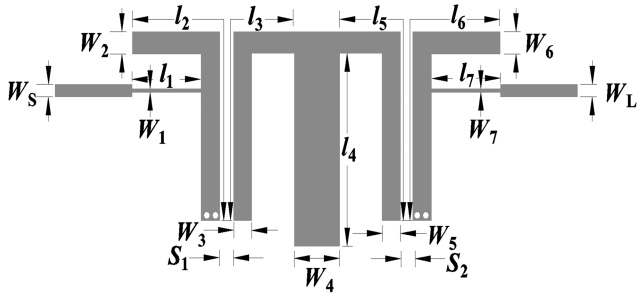

FIGURE 5. Example of the proposed bandpass filter.

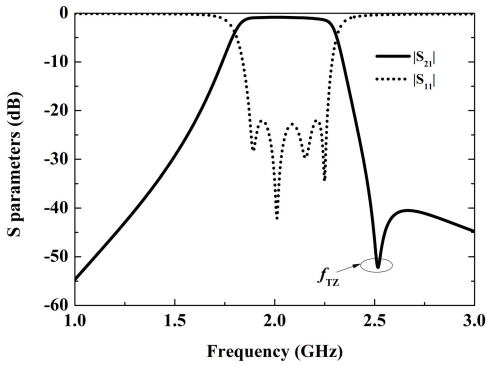

FIGURE 6. Simulated results of the proposed bandpass filter.

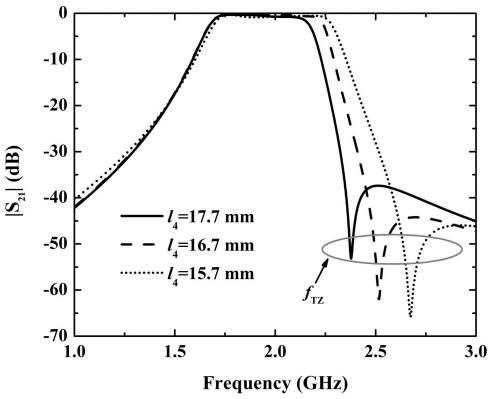

FIGURE 7. Shifting the transmission zero by changing the length l_4.

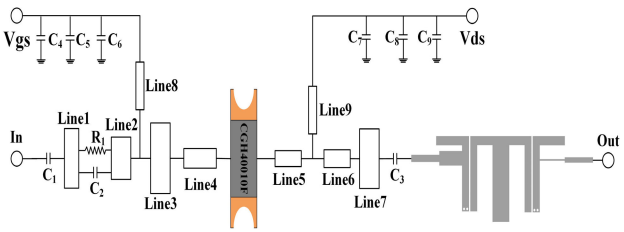

FIGURE 8. Schematic prototype of the proposed FPA.

respectively. The open-end stub with Z_4 and θ_4 is represented by the impedance inverter K_{23}. It can realize mixed coupling, and then generate a transmission zero at the frequency where $\theta_4 = \pi/2$. According to the equivalent circuit in Fig. 4, it can realize a fourth-order general Chebyshev bandpass response with one transmission zero at finite frequency.

The design procedure of the proposed filter is summarized as follows. According to filter specifications, the equivalent circuit in Fig. 4 is synthesized first by conventional filter synthesis technique, and its element values are determined. Then, according to the equivalence relations between the element values of the equivalent circuit and the electric parameters of the proposed microstrip filter, the latter is obtained from the former. If a substrate is chosen, a set of structural parameters of the proposed filter can be obtained and act as initial ones for full-wave optimization. They will be adjusted within their vicinities until final performance of the proposed microstrip filter meets requirement.

For demonstration, an example of the proposed filter is designed, as shown in Fig. 5. The substrate Rogers 4350 ($\varepsilon_r = 3.66$, h = 0.508 mm, and tan $\sigma = 0.004$) is used. The center frequency of the example is 2.0 GHz and the fractional bandwidth is 20%. Correspondingly, the structural parameters of the example are (unit: mm): $W_S = W_L = 1.1$, $l_1 = l_7 = 7.2$, $W_1 = W_7 = 0.3$, $l_2 = l_6 = 25.6$, $W_2 = W_6 = 2$, $l_3 = l_5 = 20.5$, $W_3 = W_5 = 1.9$, $l_4 = 16.7$, $W_4 = 4.9$, and $S_1 = S_2 = 0.13$, respectively. The simulated results are shown in Fig. 6. Obviously, four transmission poles are distinguished. There is one transmission zero near to the right side of the passband. By changing the length l_4 of the open-end stub, the transmission zero can be easily shifted, as shown in Fig. 7. Undoubtedly, such verifies our prediction.

B. FPA INCORPORATING THE PROPOSED BANDPASS FILTER

As shown in Fig. 1(b), the FPA includes four parts: bias network, IMN, transistor and OMN realized by BPF. One schematic prototype is shown in Fig. 8, in which the proposed filter will act as OMN. In Fig. 8, the bias network is composed of bypass capacitors C_4, C_5, C_6, C_7, C_8, and C_9, and quarter-wavelength high-impedance microstrip line *Line* 8 and 9. IMN consists of *Line* 1, 2, 3, 4, C_1, C_2 and R_1. *Line* 1, 2, 3 and 4 are mainly responsible for input matching. C_1 is a DC blocking capacitor. R_1 and C_2 constitutes stable network. For OMN, the proposed filter in the previous section is incorporated, which plays the role of filtering and impedance matching simultaneously. It is connected to the right side of the transistor through *Line* 5, 6, 7 and a DC blocking capacitor C_3. The input impedance of the filter should match the load pull matching of the transistor. Thus, *Line* 6 and 7 are used for fine tuning. *Line* 5 mainly acts as a welding plate.

To obtain high efficiency for the FPA, it is necessary to select proper fundamental load impedance. At the same time, high-order harmonic load impedances will also have a non-ignorable impact on both output power and efficiency of the FPA. Ideally, all of them should be taken into consideration. In practice, the effect of high-order harmonic load impedances will decrease as order increases. Therefore, only the second-, third- and fourth-order harmonic load

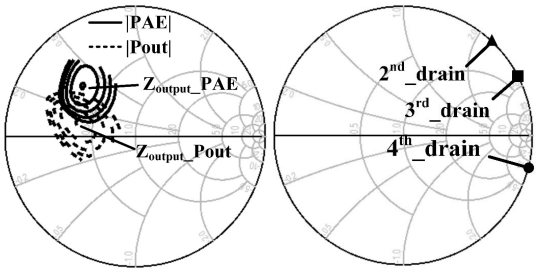

FIGURE 9. Results of fundamental and high-order harmonic load impedance pull.

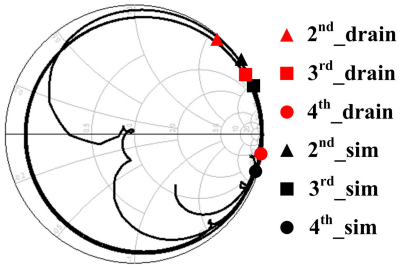

FIGURE 10. Ideal and simulated high-order harmonic load impedances.

impedances are considered in our design. Here, the multiple harmonic traction method is applied for such purpose.

For demonstration, a FPA example is designed. The center frequency is set at 2.0 GHz. This example uses a GaN transistor CGH40010F. The drain voltage is set to 28 V and the gate voltage is -3 V. The fundamental and high-order harmonic load impedances obtained by multiple harmonic traction are shown in Fig. 9. For this example, the fundamental load impedance is $15 + j13$, and the high-order harmonic ones are concentrated in the right half of Smith chart. The source impedance obtained by source traction is $6.5 + j8.8$.

For output matching, the input impedance of the proposed filter is adjusted according to the result of transistor load pull. The results of ideal and simulated high-order harmonic load impedance are shown in Fig. 10. The input impedance of the filter is required to match the high-order harmonic load impedances of the transistor. Apart from it, *Line* 6 and 7 can be tuned for better matching.

III. EXPERIMENT AND DISCUSSION

In order to verify the validity of the proposed bandpass filter and FPA, two examples were designed, fabricated and measured. Here, the substrate Rogers 4350 was still used.

A. FILTER MEASUREMENT

For demonstration, the source/load impedances of the designed filter are set as 50 Ω for easy measurement. The photo of the fabricated filter is shown in Fig. 11. Both simulated and measured results are shown in Fig. 12. The fourth-order general Chebyshev bandpass response is clearly observed. The measured center frequency is 2.0 GHz, and the 3 dB fractional bandwidth is about 20%. The minimum in-band insertion loss is 1.1 dB, and the in-band return loss

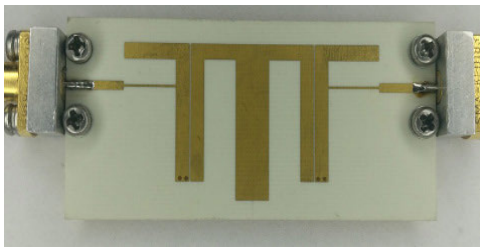

FIGURE 11. Photo of the fabricated filter.

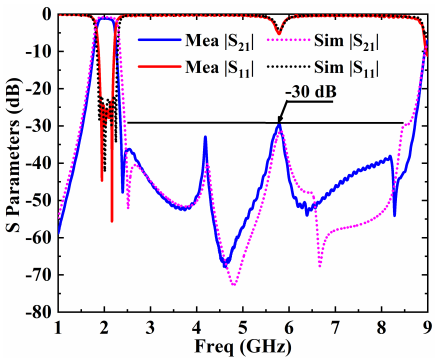

FIGURE 12. Measured and simulated S-parameters.

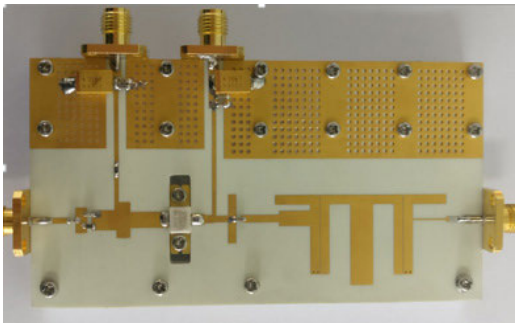

FIGURE 13. Photo of the fabricated FPA.

TABLE 1. Design parameters of the FPA example.

Parameter	Value	Parameter	Value
C_1/C_3	10 pF	*Line* 2	20 Ω/4.5 mm
C_2	10 pF	*Line* 3	12 Ω/2.7 mm
C_4/C_9	10 μF	*Line* 4	24 Ω/7.9 mm
C_5/C_8	100 pF	*Line* 5	33 Ω/2 mm
C_6/C_7	10 pF	*Line* 6	45 Ω/2.5 mm
R_1	10 Ω	*Line* 7	9 Ω/1.6 mm
Line 1	16 Ω/2.2 mm	*Line* 8/9	60 Ω/21.7 mm

is greater than 23 dB. The transmission zero created by the open-end stub is at 2.45 GHz. As high as 30 dB suppression can be achieved over 4th harmonic.

B. FPA MEASUREMENT

The photo of the fabricate FPA is shown in Fig. 13. The size of the FPA is 95 mm*50 mm. The design parameters are tabulated in Table 1. Agilent vector network analyzer was used for small-signal measurement. The measured results

TABLE 2. Comparison between the proposed FPA and others.

Ref	Filter type	Transistor	Max PAE	60%PAE bandwidth	Harmonic suppression	40 dB Rectangle coefficient
[16]	SIW	GaN	68	70MHz @3.1GHz	NA	5.6
[17]	Dielectric	GaN	70.7	30MHz @1.88GHz	NA	NA
[18]	Microstrip	LDMOS	46.3	NA	2nd	NA
[19]	Microstrip	GaN	69.8	NA	NA	NA
[20]	Hybrid cavity-Microstrip	GaN	70.9	130MHz @2.4GHz	3rd	3.4
This work	Microstrip	GaN	62	100MHz @2GHz	4th	2.5

SIW: substrate integrated waveguide.

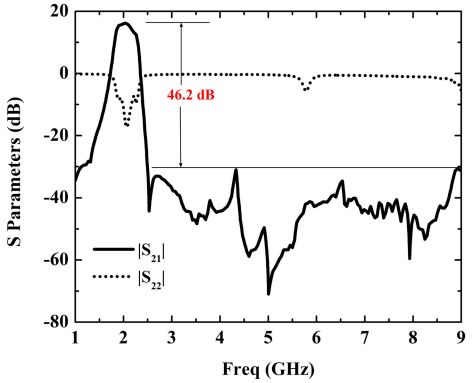

FIGURE 14. Measured S-parameters under small signal excitation.

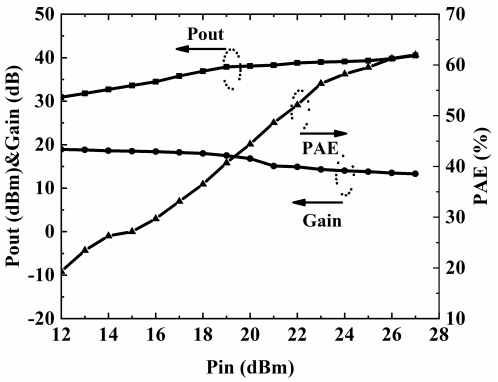

FIGURE 16. Measured PAE, Pout and Gain versus input power variation.

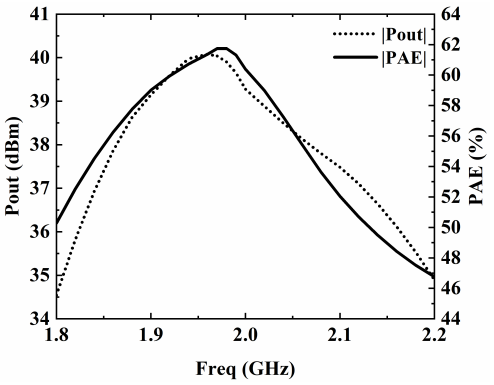

FIGURE 15. Measured Pout and PAE versus frequency.

are shown in Fig. 14. The predicted bandpass response is exhibited, and the in-band small-signal gain is about 16.2 dB. A transmission zero is generated at 2.5 GHz, which is near the passband. So sharp selectivity is achieved. As high as 46.2 dB out-of-band suppression is also achieved and extended over the fourth-order harmonic.

The large-signal measurement results are shown in Fig. 15, which depicts the curve of Pout and PAE (power-added efficiency) versus frequency. The measured maximum PAE is 62%, and the maximum Pout is 40.5 dBm. More than 60% PAE is achieved over from 1.92 GHz to 2.02 GHz. Fig. 16 shows the measured Pout, Gain, and PAE for input power from 12 dBm to 28 dBm at a center frequency of 2.0 GHz.

In order to demonstrate the advantages of the proposed FPA, it is compared with others from some literatures in Table 2. Clearly, the proposed FPA is featured by wide bandwidth, relatively high efficiency, sharp selectivity and excellent harmonic suppression.

IV. CONCLUSION

This paper presents a novel FPA with capability of power amplification and filtering. Unlike conventional PA and filter that are treated as separate two components. The proposed FPA incorporating a novel bandpass filter as part of its output matching network, which is advantageous to whole performance optimization and miniaturization. As verified by measurement, the proposed FPA is featured by sharp selectivity and high harmonic suppression, and other advantages such as high power-added efficiency and wide bandwidth is still retained. As demonstrated in this paper, integration design of conventional separate components will bring some advantages such as size reduction, whole performance optimization, etc.

REFERENCES

[1] K. Song, F. Zhang, S. Hu, and Y. Fan, "Ku-band 200-W pulsed power amplifier based on waveguide spatially power-combining technique for industrial applications," *IEEE Trans. Ind. Electron.*, vol. 61, no. 8, pp. 4274–4280, Aug. 2014.

[2] S. Y. Zheng, Z. W. Liu, X. Y. Zhang, X. Y. Zhou, and W. S. Chan, "Design of ultrawideband high-efficiency extended continuous class-F power amplifier," *IEEE Trans. Ind. Electron.*, vol. 65, no. 6, pp. 4661–4669, Jun. 2018.
[3] A. Sheikhi, M. Hayati, and A. Grebennikov, "High-efficiency class-E and class-F/E power amplifiers at any duty ratio," *IEEE Trans. Ind. Electron.*, vol. 63, no. 2, pp. 840–848, Feb. 2016.
[4] K. Chen and D. Peroulis, "Design of broadband highly efficient harmonic-tuned power amplifier using in-band continuous class-F^{-1}/F mode transferring," *IEEE Trans. Microw. Theory Techn.*, vol. 60, no. 12, pp. 4107–4116, Dec. 2012.
[5] F. J. Martinez-Rodriguez, P. Roblin, Z. Popovic, and J. I. Martinez-Lopez, "Optimal definition of class f for realistic transistor models," *IEEE Trans. Microw. Theory Techn.*, vol. 65, no. 10, pp. 3585–3595, Oct. 2017.
[6] F. You and J. Benedikt, "An optimized-load-impedance calculation and mining method based on I–V Curves: Using broadband class-E power amplifier as example," *IEEE Trans. Ind. Electron.*, vol. 66, no. 7, pp. 5254–5263, Jul. 2019.
[7] Z. Dai, S. He, J. Peng, C. Huang, W. Shi, and J. Pang, "A semianalytical matching approach for power amplifier with extended chebyshev function and real frequency technique," *IEEE Trans. Microw. Theory Techn.*, vol. 65, no. 10, pp. 3892–3902, Oct. 2017.
[8] P. Jia, F. You, S. He, and X. Qian, "A 0.25–1.25-GHz high-efficiency power amplifier with computer-aided design based on optimized impedance solution continuum," *IEEE Microw. Wireless Compon. Lett.*, vol. 28, no. 5, pp. 443–445, May 2018.
[9] K. Rawat and F. M. Ghannouchi, "Design methodology for dual-band Doherty power amplifier with performance enhancement using dual-band offset lines," *IEEE Trans. Ind. Electron.*, vol. 59, no. 12, pp. 4831–4842, Dec. 2012.
[10] J. Kim, "Highly efficient asymmetric class-F^{-1}/F GaN Doherty amplifier," *IEEE Trans. Microw. Theory Techn.*, vol. 66, no. 9, pp. 4070–4077, Sep. 2018.
[11] J. Wang, S. He, F. You, W. Shi, J. Peng, and C. Li, "Codesign of high-efficiency power amplifier and ring-resonator filter based on a series of continuous modes and even–odd-mode analysis," *IEEE Trans. Microw. Theory Techn.*, vol. 66, no. 6, pp. 2867–2878, Jun. 2018.
[12] S. Sadjina, R. S. Kanumalli, A. Gebhard, K. Dufrene, M. Huemer, and H. Pretl, "A mixed-signal circuit technique for cancellation of interferers modulated by LO phase-noise in 4G/5G CA transceivers," *IEEE Trans. Circuits Syst. I, Reg. Papers*, vol. 65, no. 11, pp. 3745–3755, Nov. 2018.
[13] P. Orsatti, F. Piazza, and Q. Huang, "A 20-mA-receive, 55-mA-transmit, single-chip GSM transceiver in 0.25-μm CMOS," *IEEE J. Solid-State Circuits*, vol. 34, no. 12, pp. 1869–1880, Dec. 1999.
[14] A. Gebhard, O. Lang, M. Lunglmayr, C. Motz, R. S. Kanumalli, C. Auer, T. Paireder, M. Wagner, H. Pretl, and M. Huemer, "A robust nonlinear RLS type adaptive filter for second-order-intermodulation distortion cancellation in FDD LTE and 5G direct conversion transceivers," *IEEE Trans. Microw. Theory Techn.*, vol. 67, no. 5, pp. 1946–1961, May 2019.
[15] H. Zheng, S. Lou, D. Lu, C. Shen, T. Chan, and H. C. Luong, "A 3.1 GHz–8.0 GHz single-chip transceiver for MB-OFDM UWB in 0.18-μm CMOS process," *IEEE J. Solid-State Circuits*, vol. 44, no. 2, pp. 414–426, Feb. 2009.
[16] K. Chen, J. Lee, W. J. Chappell, and D. Peroulis, "Co-design of highly efficient power amplifier and high-Q output bandpass filter," *IEEE Trans. Microw. Theory Techn.*, vol. 61, no. 11, pp. 3940–3950, Nov. 2013.
[17] J.-X. Xu, X. Y. Zhang, and X.-Q. Song, "High-efficiency filter-integrated class-f power amplifier based on dielectric resonator," *IEEE Microw. Wireless Compon. Lett.*, vol. 27, no. 9, pp. 827–829, Sep. 2017.
[18] Y. C. Li, K. C. Wu, and Q. Xue, "Power amplifier integrated with bandpass filter for long term evolution application," *IEEE Microw. Wireless Compon. Lett.*, vol. 23, no. 8, pp. 424–426, Aug. 2013.
[19] L. Gao, X. Y. Zhang, S. Chen, and Q. Xue, "Compact power amplifier with bandpass response and high efficiency," *IEEE Microw. Wireless Compon. Lett.*, vol. 24, no. 10, pp. 707–709, Oct. 2014.
[20] Q.-Y. Guo, X. Y. Zhang, J.-X. Xu, Y. C. Li, and Q. Xue, "Bandpass Class-F power amplifier based on multifunction hybrid cavity–microstrip filter," *IEEE Trans. Circuits Syst. II, Exp. Briefs*, vol. 64, no. 7, pp. 742–746, Jul. 2017.

XIAOBO QI is currently pursuing the master's degree under the supervision of Prof. F. Xiao.

FEI XIAO (Member, IEEE) received the M.Sc. and Ph.D. degrees from the University of Electronic Science and Technology of China (UESTC), in 2002 and 2005, respectively. From 2009 to 2010, he was a Visiting Researcher with the Royal Institute of Technology, Sweden, and the University of Birmingham, U.K., from 2015 to 2016. He is currently a Professor with UESTC. Until now, he has authored over 100 journal and conference papers. He holds 18 authorized patents. His research interests include filter synthesis, microwave passive components design, and computational electromagnetics.